Breaking of nucleon Cooper pairs at finite temperature in $^{93-98}$Mo

K. Kaneko,[1] M. Hasegawa,[2] U. Agvaanluvsan,[3, 4] E. Algin,[3, 4, 5, 6] R. Chankova,[7] M. Guttormsen,[7]
A.C. Larsen,[7] G.E. Mitchell,[4, 5] J. Rekstad,[7] A. Schiller,[8] S. Siem,[7] and A. Voinov[9]

[1]*Department of Physics, Kyushu Sangyo University, Fukuoka 813-8503, Japan*
[2]*Laboratory of Physics, Fukuoka Dental College, Fukuoka 814-0193, Japan*
[3]*Lawrence Livermore National Laboratory, L-414, 7000 East Avenue, Livermore, CA 94551, USA*
[4]*North Carolina State University, Raleigh, NC 27695, USA*
[5]*Triangle Universities Nuclear Laboratory, Durham, NC 27708, USA*
[6]*Department of Physics, Osmangazi University, Meselik, Eskisehir, 26480 Turkey*
[7]*Department of Physics, University of Oslo, N-0316 Oslo, Norway*
[8]*NSCL, Michigan State University, East Lansing, MI 48824, USA*
[9]*Department of Physics and Astronomy, Ohio University, Athens, OH 45701, USA*
(Dated: February 9, 2008)

The $\mathcal{S}$ shape of the canonical heat capacity is known as a signature of the pairing transition and along an isotopic chain it is significantly more pronounced for nuclei with an even number of neutrons than with an odd number. Although the heat capacities extracted from experimental level densities in $^{93-98}$Mo exhibit a clear $\mathcal{S}$ shape, they do not show such an odd-even staggering. To understand the underlying physics, we analyze thermal quantities evaluated from the partition function calculated using the static-path plus random-phase approximation (SPA+RPA) in a monopole pairing model with number-parity projection. The calculated level densities reproduce very well the experimental data and they also agree with estimates using the back-shifted Fermi-gas model. We clarify the reason why the heat capacities for Mo isotopes do not show odd-even staggering of the $\mathcal{S}$ shape. We also discuss thermal odd-even mass differences in $^{94-97}$Mo using the three-, four-, and five-point formula. These thermal mass differences are regarded as indicators of pairing correlations at finite temperature.

PACS numbers: 21.60.Jz, 21.10.Ma, 05.30.-d

Level density is one of the basic ingredients required for theoretical studies of nuclear structure and reactions. Recently, level densities for $^{93-98}$Mo [1] have been extracted by the group at the Oslo Cyclotron Laboratory. In their paper, the $\mathcal{S}$ shape of the canonical heat capacity is interpreted as consistent with a pairing phase transition with a critical temperature for the quenching of pairing correlations of $T_c \sim 0.7$–1.0 MeV.

Pairing correlations are of special importance in nuclear physics. The Bardeen-Cooper-Schrieffer (BCS) theory [2] has successfully described the sharp phase transition connected to the breakdown of pairing correlations for infinite Fermi system of electrons in low-temperature superconductors. This sharp phase transition leads to a discontinuity of the heat capacity at the critical temperature, which indicates a second-order phase transition. For finite Fermi systems such as the atomic nucleus, however, nucleon number fluctuations and thermal and quantal fluctuations beyond the mean field become large. These fluctuations wash out the discontinuity of the heat capacity in the mean-field approximation and give rise to an $\mathcal{S}$ shape [3]. In recent theoretical approaches such fluctuations have been taken into account. Examples are: the static-path plus random-phase approximation (SPA+RPA) [3] and shell-model Monte-Carlo (SMMC) calculations [4, 5, 6].

It has recently been reported [7, 8] that the canonical heat capacities extracted from experimental level densities exhibit $\mathcal{S}$ shapes with a peak around the critical temperature. The $\mathcal{S}$ shape is well correlated with the suppression of the number of spin-zero pairs around the critical temperature [5, 6]. The important feature is an odd-even staggering of the $\mathcal{S}$ shape where the $\mathcal{S}$ shape of the heat capacity for an even number of neutrons is significantly more pronounced than the one for an odd number of neutrons [3, 5, 7]. A shell-model analysis [5, 6, 9] suggests that the difference between heat capacities of nuclei with even and odd numbers of neutrons is an important measure for understanding the breaking of neutron pairs. Figure 1 shows the experimental level densities for $^{93-98}$Mo [1]. The extrapolated level densities using the back-shifted Fermi-gas model shown in Fig. 2 make it possible to systematically study pairing correlations at finite temperatures in a series of odd- and even-mass nuclei. The heat capacities extracted from experimental level densities all show a clear $\mathcal{S}$ shape as seen in Fig. 3. Therefore, the heat capacities of $^{93-98}$Mo reveal a systematic, different from that of other experimental data [7, 8] and theoretical calculations [3, 5, 6].

The $\mathcal{S}$ shape of the heat capacity around the critical temperature is not a quantity which reflects details of the pairing transition. We cannot distinguish between, e.g., quenching of proton-proton (pp) and neutron-neutron (nn) pairing correlations from the $\mathcal{S}$ shape. In our recent papers [9, 10, 11], we demonstrated that the suppression of pairing correlations around the critical temperature appears in thermal odd-even mass differences using the three-point formula. For heated systems, the thermal odd-even mass difference is the natural extension of the odd-even mass difference [12, 13, 14] observed for nuclear
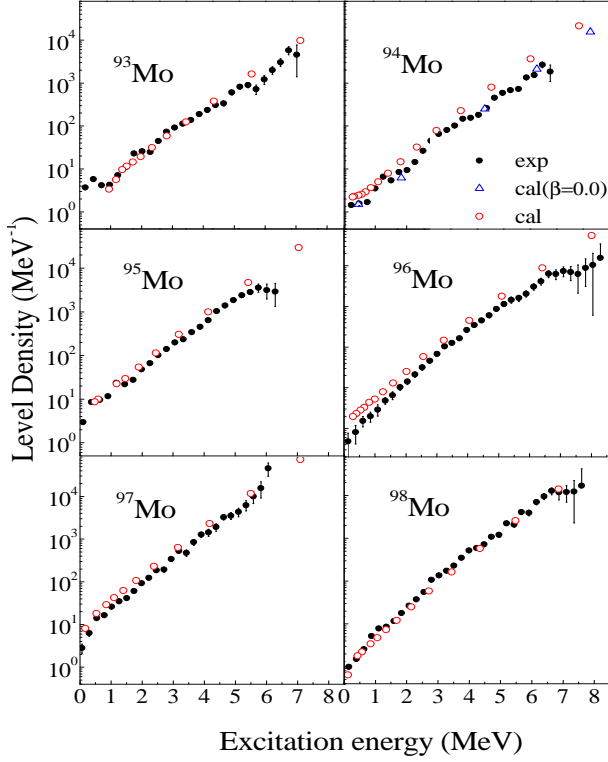
FIG. 1: (Color online) Experimental and calculated level densities as a function of excitation energy in $^{93-98}$Mo [1]. The open circles denote the SPA+RPA calculations. The error bars show the statistical uncertainties.
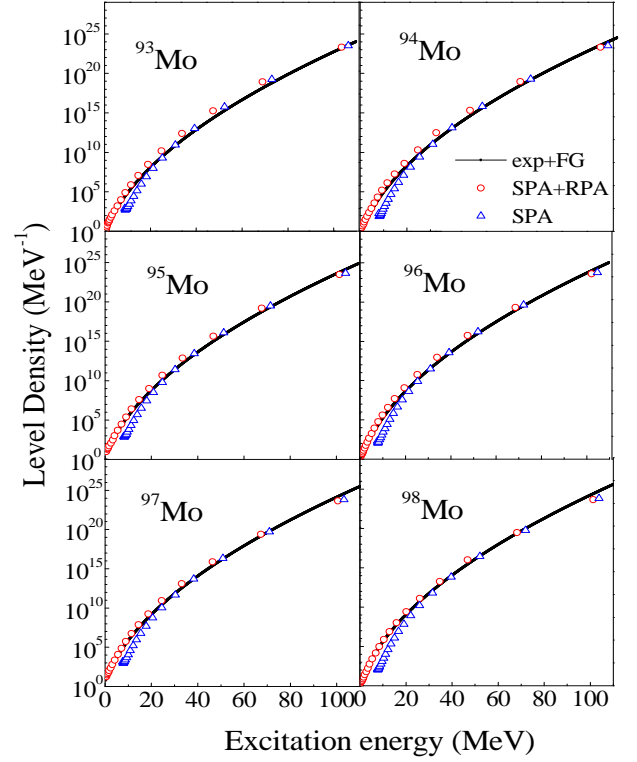

FIG. 2: (Color online) Extrapolated and calculated level densities as a function of excitation energy in $^{93-98}$Mo. The open circles and triangles denote the SPA+RPA and SPA calculations, respectively.

ground-state masses.

The aim of this rapid communication is to investigate pairing properties in $^{93-98}$Mo. We report on SPA+RPA calculations in the monopole pairing model using a deformed Woods-Saxon potential with spin-orbit interaction [15] and we discuss physical reasons for why the heat capacities for Mo isotopes do not show an odd-even staggering of the $\mathcal{S}$ shape.

Let us start from a monopole pairing Hamiltonian

$$H = \sum_{k,\tau} \varepsilon_{k,\tau}(c^\dagger_{k,\tau}c_{k,\tau} + c^\dagger_{\bar{k},\tau}c_{\bar{k},\tau}) - \sum_\tau G_\tau P^\dagger_\tau P_\tau, \quad (1)$$

where $\tau = n, p$ and $\bar{k}$ denotes the time reversed state. Here, $\varepsilon_{k,\tau}$ is a single-particle energy and P_τ is the pairing operator $P_\tau = \sum_k c_{\bar{k},\tau}c_{k,\tau}$. Here, we neglect proton-neutron pairing interactions because in $^{93-98}$Mo the respective single-particle orbitals might be too far from each other to play a role. By means of the SPA+RPA [3] based on the Hubbard-Stratonovich transformation [16], the number-parity projected partition function is given by

$$\begin{aligned} Z^{\mathrm{c}} &= \mathrm{Tr}\left[P_N P_Z e^{-H/T}\right]_{\mathrm{SPA+RPA}} \\ &= \prod_\tau \frac{2}{G_\tau T}\int_0^\infty \Delta_\tau d\Delta_\tau e^{-\Delta_\tau^2/G_\tau T} Z_\tau C^\tau_{\mathrm{RPA}} \quad (2) \end{aligned}$$

with

$$\begin{aligned} Z_\tau &= \frac{1}{2}\prod_k e^{-\gamma_{k,\tau}/T}\left(1 + e^{-\lambda_{k,\tau}/T}\right)^2 \\ &\quad \times \left[1 + \sigma\prod_{k'}\tanh^2(\lambda_{k',\tau}/T)\right] \quad (3) \end{aligned}$$

and

$$C^\tau_{\mathrm{RPA}} = \prod_k \frac{\omega_{k,\tau}\sinh[\lambda_{k,\tau}/T]}{2\lambda_{k,\tau}\sinh[\omega_{k,\tau}/2T]} \quad (4)$$

where, instead of the exact number projection, we introduced the number-parity projections $P_N = (1+\sigma e^{i\pi N})/2$ for neutron number N and $P_Z = (1+\sigma e^{i\pi Z})/2$ for proton number Z (σ denotes the even or odd number parity [3]). It has recently been shown that in the monopole pairing case the SPA+RPA with number-parity projection reproduces well exact results [3]. The number-parity projection is essential to describe thermal properties at low temperature. Here, we use the notation $\omega_{k,\tau}$ for the conventional thermal RPA energies and $\lambda_{k,\tau} = \sqrt{\varepsilon'^2_{k,\tau} + \Delta^2_\tau}$, $\varepsilon'_{k,\tau} = \varepsilon_{k,\tau} - \mu_\tau - G_\tau/2$, and $\gamma_{k,\tau} = \varepsilon_{k,\tau} - \mu_\tau - \lambda_{k,\tau}$. The SPA partition function is obtained by neglecting the RPA partition function C^τ_{RPA}. The thermal energy can be calculated from $E = -\partial \ln Z^{\mathrm{c}}/\partial\beta$ where
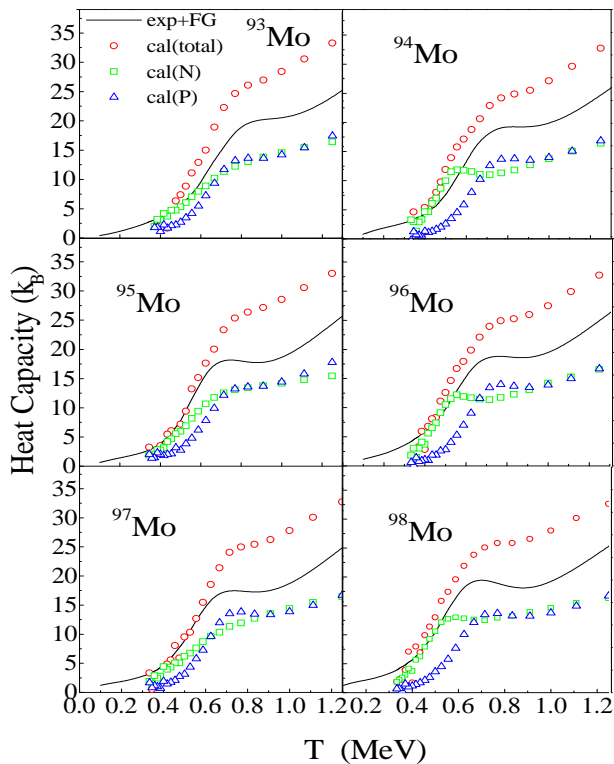
FIG. 3: (Color online) Heat capacities as a function of temperature T in $^{93-98}$Mo. The solid curve denotes the heat capacity extracted from the experimental level density. The open squares and open triangles are the calculated heat capacities for neutrons and protons, respectively. The total heat capacities are represented by the open circles.

$\beta = 1/T$. In this work, we use the single-particle energies $\varepsilon_{k,\tau}$ given by an axially deformed Woods-Saxon potential with spin-orbit interaction. We choose the Woods-Saxon parameters of [15], where $V_0 = 51.0$ MeV, $a = 0.67$ fm, $\kappa = 0.67$, $\lambda = 20.3$, and $r_0 = 1.27$ fm. We have calculated the single-particle spectrum of this potential, and used it to compute the number-parity projected partition function. The deformation parameters for the even-even nuclei ^{94,96,98}Mo are estimated from the experimental $B(E2; 2_1^+ \rightarrow 0_1^+)$ values, and are determined as $\beta_2 = 0.15$, 0.17, and 0.17, respectively. Those for the odd nuclei ^{93,95,97}Mo are chosen as $\beta_2 = 0.10$, 0.08, and 0.17, respectively. The 25 and 30 doubly degenerate single-particle levels with negative energy are taken with respect to neutrons and protons outside the ^{48}Ca core. The positive energy levels (resonances and continuum states) are neglected [6]. We adjusted the pairing force strengths at $G_n = 22/A$ MeV for neutrons and $G_p = 26.5/A$ MeV for protons in order to reproduce the three-point odd-even mass differences.

The level density can be evaluated from an inverse Laplace transformation of the partition function Z^c in

TABLE I: Parameters used for the back-shifted Fermi-gas level density.

Nucleus	E_{pair} (MeV)	a (MeV^{-1})	C_1 (MeV)	η
^{98}Mo	2.080	11.33	-1.521	0.87
^{97}Mo	0.995	11.23	-1.526	0.65
^{96}Mo	2.138	11.13	-1.531	0.46
^{95}Mo	1.047	11.03	-1.537	0.34
^{94}Mo	2.027	10.93	-1.542	0.25
^{93}Mo	0.899	10.83	-1.547	0.08

the saddle-point approximation as

$$\rho(E) \approx \frac{Z^c e^{\beta E}}{[2\pi \partial^2 \ln Z^c / \partial \beta^2]^{1/2}}. \tag{5}$$

The calculated level densities as a function of thermal energy are shown in Fig. 1, where the calculated level density is also plotted for $\beta_2 = 0$. The calculations reproduce very well the experimental data. It should be noted that, more precisely, Eq. (5) gives the state density and not the level density because the partition function Z^c in Eq. (2) includes m-degeneracy [1]. This difference may have an impact on the canonical heat capacity.

We now extrapolate the experimental level densities by the back-shifted Fermi-gas model of [17, 18]

$$\rho_{\text{BSFG}}(E) = \eta \frac{\exp\left[2\sqrt{aU}\right]}{12\sqrt{2}a^{1/4}U^{5/4}\sigma_I}, \tag{6}$$

where the back-shifted energy is $U = E - E_1$ and the spin-cutoff parameter σ_I is taken as $\sigma_I^2 = 0.0888A^{2/3}\sqrt{aU}$. The level-density parameter a and the parameter E_1 are given by $a = 0.21A^{0.87}$ MeV^{-1} and $E_1 = C_1 + E_{\text{pair}}$, respectively, where the back-shift is parameterized by $C_1 = -6.6A^{-0.32}$ MeV and the pairing energy E_{pair} is based on pairing-gap parameters $\Delta_n^{(3)}$ and $\Delta_p^{(3)}$ evaluated from odd-even mass differences [13]. The factor η is introduced in order to reproduce experimental neutron-resonance spacings. The parameters used for $^{93-98}$Mo are listed in Table I. Figure 2 displays the extrapolated and calculated level densities as a function of excitation energy. The level densities from the SPA+RPA calculation are in good agreement with the extrapolated ones. In Fig. 2, we also compare the SPA+RPA with the pure SPA calculation. It is noted, that because of the RPA contributions, the calculated level density is significantly increased below an excitation energy of ~ 20 MeV.

To study thermal properties derived from experimental level densities, let us start from the partition function in the canonical ensemble, i.e., the Laplace transform of the
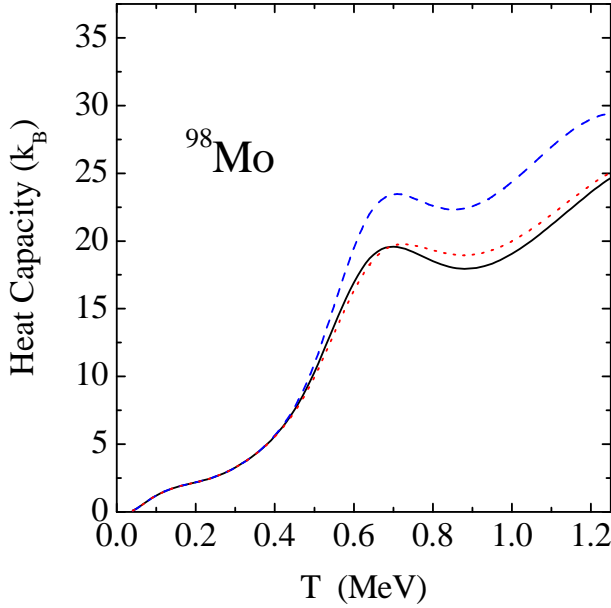
FIG. 4: (Color online) Heat capacities derived using different extrapolations of the experimental level-density curve in ^{98}Mo. The extrapolations are performed with a 20% increase of (i) the level-density parameter (dashed line) or (ii) the pairing-gap parameter (dotted line), respectively. The solid curve indicates the heat-capacity curve of Fig. 3.

level density $\rho(E_i)$

$$Z(T) = \sum_{i=0}^{\infty} \delta E_i \rho(E_i) \mathrm{e}^{-E_i/T}, \qquad (7)$$

where E_i are the excitation energies and δE_i are the energy bins. Then, the thermal energy is expressed as

$$E(Z, N, T) = \sum_{i=0}^{\infty} \delta E_i \rho(E_i) E_i \mathrm{e}^{-E_i/T}/Z(T), \qquad (8)$$

and the heat capacity is given by

$$C(Z, N, T) = \frac{\partial E(Z, N, T)}{\partial T}. \qquad (9)$$

Formally, the calculations using Eqs. (7)–(9) require an infinite summation. However, the experimental level densities in Fig. 1 only cover the excitation energy up to 6.0–8.5 MeV. Since the calculated level densities agree well with those extrapolated using the back-shifted Fermi-gas model of Eq. (6), we use this extrapolation to extend the experimental level-density data up to an excitation energy of ∼180 MeV before evaluating Eqs. (7)–(9). The $\mathcal{S}$-shape behavior of the heat capacities for $^{93-98}$Mo can be reproduced by the calculation, although the calculated heat capacities are larger than the experimental ones above the critical temperature. The characteristic feature is that all of the nuclei $^{93-98}$Mo exhibit a clear $\mathcal{S}$ shape of the heat capacity around the critical temperature $T_c \sim 0.7$–0.9 MeV. The calculated heat capacities
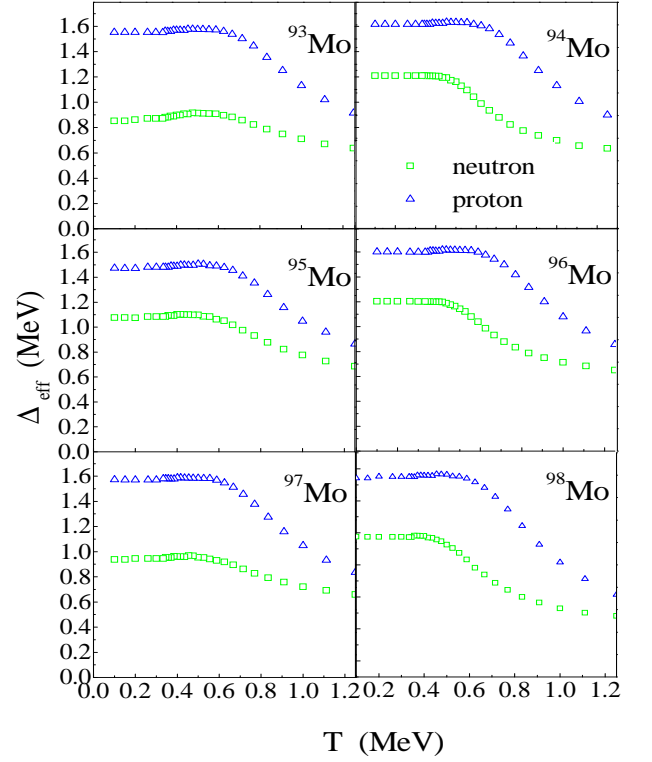

FIG. 5: (Color online) Effective pairing gap as a function of temperature. The open squares and open triangles denote the effective pairing gaps for neutrons and protons, respectively.

are divided into neutron and proton parts as shown in Fig. 3. This figure also indicates that the heat capacity for the neutron part shows a different behavior from the one for the proton part. For the neutron part, the critical temperature is ~ 0.55 MeV and the $\mathcal{S}$ shape of the heat capacity for an even number of neutrons is more pronounced than the one for an odd number of neutrons. For the proton part, on the other hand, the heat capacities show the same clear $\mathcal{S}$ shape around $T_c \sim 0.75$ MeV for all of the nuclei $^{93-98}$Mo. Thus, we conclude that the experimentally observed $\mathcal{S}$ shape of the heat capacity in $^{93-98}$Mo can be attributed mainly to the proton contribution.

We will now discuss how sensitive the extracted heat capacities in Fig. 3 are with respect to the level-density extrapolation. Figure 4 shows the extracted heat capacities using a 20% larger (i) level-density parameter a or (ii) pairing-gap parameter E_{pair}. The increased a makes the slope of the heat-capacity curve steeper than before; the increase of the pairing-gap parameter does not change the heat-capacity curve significantly. In either case, the heat capacity shows a pronounced $\mathcal{S}$ shape which indicates that this qualitative feature is very robust with respect to changes in the Fermi-gas parameters of the level-density extrapolation.

The $\mathcal{S}$ shape has been discussed to be correlated with the breaking of nucleon Cooper pairs [5, 9]. Therefore, we further investigate the pairing properties in the calcu-
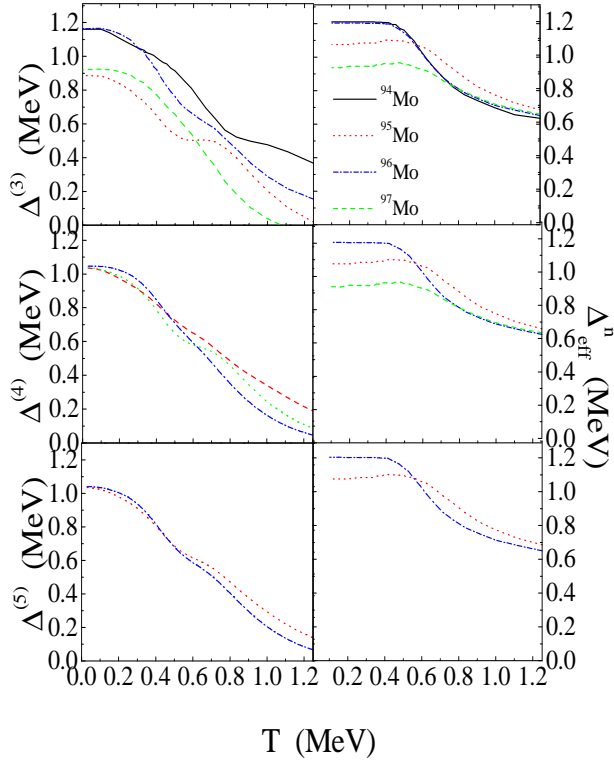
FIG. 6: (Color online) Left: thermal pairing gaps extracted from the three-, four-, and five-point indicators of the thermal odd-even mass difference as a function of temperature. Right: effective pairing gaps for neutrons in the monopole-pairing-model calculations of this work.

lations. Figure 5 shows the effective pairing gap defined by

$$\Delta_{eff}^{\tau} = G_{\tau} \left[\frac{1}{\beta} \frac{\partial \ln Z^c}{\partial G_{\tau}} \right]^{1/2}. \tag{10}$$

Around $T_c \sim 0.6$ MeV, Δ_{eff}^n decreases more rapidly for an even number of neutrons than for an odd number of neutrons. The suppression of Δ_{eff}^n is well correlated with the $\mathcal{S}$ shape of the heat capacity for neutrons in Fig. 3. Furthermore, Δ_{eff}^p decreases drastically around $T_c \sim 0.8$ MeV for all of the nuclei $^{93-98}$Mo. This suppression of Δ_{eff}^p correlates well in temperature with the pronounced $\mathcal{S}$ shape of the proton heat capacity in Fig. 3. Thus, the $\mathcal{S}$ shape in Fig. 3 can be understood in terms of the suppression of the effective pairing gap.

The ground-state odd-even mass difference is known to be a measure of pairing correlations [12, 14]. Extending this odd-even mass difference, we have proposed the thermal odd-even mass difference as a measure of pairing correlations at finite temperatures [9, 10]. The three-point thermal odd-even mass difference for neutrons is given by

$$\Delta_n^{(3)}(Z,N,T) = \frac{(-1)^N}{2} \left[B_t(Z,N+1,T) \right.$$
$$\left. -2B_t(Z,N,T) + B_t(Z,N-1,T) \right], \tag{11}$$

where the thermal energy B_t is defined by $B_t(Z,N,T) = E(Z,N,T) + B(Z,N)$ and $B(N,Z)$ is the binding energy at zero temperature. The thermal odd-even mass difference $\Delta_n^{(3)}$ is evaluated using $E(Z,N,T)$ from Eq. (8). In our previous work [10], we extracted the thermal odd-even mass difference $\Delta_n^{(3)}$ in ^{184}W from the experimental level densities of ^{183}W, ^{184}W, and ^{185}W, and we obtained a drastic decrease of $\Delta_n^{(3)}$ at the critical temperature, a signal which can be correlated to a corresponding $\mathcal{S}$ shape of the heat capacity. As we have already mentioned in Ref. [10], the sudden decrease of the thermal odd-even mass differences is interpreted as a rapid breaking of nucleon Cooper pairs. It is therefore interesting to see whether such a drastic change is found for the Mo isotopes as well.

The upper left panel of Fig. 6 shows the thermal odd-even mass differences $\Delta_n^{(3)}$ for neutrons as a function of temperature. For ^{94}Mo, $\Delta_n^{(3)}$ starts to decrease rather suddenly around $T = 0.6$ MeV, however, this decrease is never as drastic as the one observed for ^{184}W [10]. Moreover, for $^{95-97}$Mo the thermal odd-even mass differences $\Delta_n^{(3)}$ do not display any sudden onset of quenching, rather they exhibit a more monotonous decrease with increasing temperature starting as early as around $T = 0.2$ MeV. We now compare these thermal odd-even mass differences $\Delta_n^{(3)}$ to the effective pairing gaps Δ_{eff}^n for neutrons in the monopole-pairing-model calculations for $^{94-97}$Mo (upper right panel of Fig. 6). The calculated effective pairing gaps decrease suddenly around the critical temperature corresponding to the presence of the $\mathcal{S}$ shape in the heat-capacity curves. At high temperatures of $T = 1.25$ MeV, their values are $\Delta_{eff}^n = 0.6$–0.7 MeV which is in reasonable agreement with the thermal odd-even mass differences for ^{94}Mo, however, the thermal odd-even mass differences for $^{95-97}$Mo are much smaller than the theoretical estimates at these high temperatures.

It has been demonstrated recently that $\Delta_n^{(3)}$ contains additional mean-field contributions when realistic pairing forces are used in the calculations [14], however, the five-point odd-even mass difference $\Delta_n^{(5)}$ extracts the pairing gap. Therefore, we also calculate the four- and five-point thermal odd-even mass differences

$$\Delta_n^{(4)}(Z,N,T) = \frac{1}{2} \left[\Delta_n^{(3)}(Z,N,T) + \Delta_n^{(3)}(Z,N-1,T) \right], \tag{12}$$

and

$$\Delta_n^{(5)}(Z,N,T) = \frac{1}{4} \left[\Delta_n^{(3)}(Z,N+1,T) \right.$$
$$\left. + 2\Delta_n^{(3)}(Z,N,T) + \Delta_n^{(3)}(Z,N-1,T) \right]. \tag{13}$$

The lower left panels of Fig. 6 show the thermal odd-even mass differences for neutrons $\Delta_n^{(4,5)}$ as a function of temperature, where $\Delta_n^{(4)}$ and $\Delta_n^{(5)}$ are obtained by the same treatment as $\Delta_n^{(3)}$. The thermal odd-even mass differences $\Delta_n^{(4,5)}$ extracted from the experimental data also

show a monotonous decrease in contrast to the sudden quenching of the effective pairing gap around the critical temperature in the monopole-pairing-model calculations for $^{94-97}$Mo (lower right panels).

Thus, the majority of the thermal odd-even mass differences $\Delta_n^{(3,4,5)}$ decrease monotonously and do not show any sudden quenching, while the theoretical calculations suggest the presence of a pairing phase transition at a critical temperature of $T = 0.6$ MeV. To possibly explain this discrepancy, we would like to point out that the thermal odd-even mass differences $\Delta_n^{(3,4,5)}$ are phenomenological indicators extracted from level densities; they may include other correlations than just monopole pairing correlations. E.g., quadrupole correlations, which are not taken into account in our calculations, could be important for understanding thermal properties. Such additional seniority non-conserving correlations may wash out the expected sudden decrease of $\Delta_n^{(3,4,5)}$ due to the breaking of nucleon Cooper pairs at the critical temperature. Hence, the relation between the odd-even mass differences and the pairing correlations at finite temperature still remains an open question.

In conclusion, we have investigated pairing properties in the $^{93-98}$Mo isotopic chain of neutron-odd and -even nuclei by performing SPA+RPA calculations within a monopole pairing model. The calculations reproduce very well the experimental level densities, and explain an unusual feature recently found for $^{93-98}$Mo, namely that the corresponding heat capacities do not show any pronounced odd-even staggering. The thermal three-, four-, and five-point odd-even mass differences in $^{94-97}$Mo, which are regarded as measures of pairing correlations at finite temperature, were extracted from the experimental level densities. They show a monotonous decrease with increasing temperature and no sudden drastic quenching. Further theoretically studies in this direction are in progress. On the experimental side, we plan for further experiments to also extract proton odd-even mass differences at finite temperature. Strong quenching of proton pairing correlations as seen on Fig. 5 suggests a drastic suppression of odd-even mass differences for isotonic chains.

[1] R. Chankova *et al.*, Phys. Rev. C **73**, 034311 (2006).

[2] J. Bardeen, L. N. Cooper, and J. R. Schrieffer, Phys. Rev. **108**, 1175 (1957).

[3] R. Rossignoli, N. Canosa, and P. Ring, Phys. Rev. Lett. **80**, 1853 (1998).

[4] S. Rombouts, K. Heyde, and N. Jachowicz, Phys. Rev. C **58**, 3295 (1998).

[5] S. Liu and Y. Alhassid, Phys. Rev. Lett. **87**, 022501 (2001).

[6] Y. Alhassid, G. F. Bertsch, and L. Fang, Phys. Rev. C **68**, 044322 (2003).

[7] A. Schiller, A. Bjerve, M. Guttormsen, M. Hjorth-Jensen, F. Ingebretsen, E. Melby, S. Messelt, J. Rekstad, S. Siem, and S. W. Ødegård, Phys. Rev. C **63**, 021306(R) (2001).

[8] E. Melby, L. Bergholt, M. Guttormsen, M. Hjorth-Jensen, F. Ingebretsen, S. Messelt, J. Rekstad, A. Schiller, S. Siem, and S. W. Ødegård, Phys. Rev. Lett. **83**, 3150 (1999).

[9] K. Kaneko and M. Hasegawa, Nucl. Phys. **A740**, 95 (2004).

[10] K. Kaneko and M. Hasegawa, Phys. Rev. C **72**, 024307 (2005).

[11] K. Kaneko and M. Hasegawa, Phys. Rev. C **72**, 061306(R) (2005).

[12] W. Satuła, J. Dobaczewski, and W. Nazarewicz, Phys. Rev. Lett. **81**, 3599 (1998).

[13] J. Dobaczewski, P. Magierski, W. Nazarewicz, W. Satuła, and Z. Szymański, Phys. Rev. C **63**, 024308 (2001).

[14] T. Duguet, P. Bonche, P.-H. Heenen, and J. Meyer, Phys. Rev. C **65**, 014311 (2002).

[15] S. Cwiok, J. Dudek, W. Nazarewicz, J. Skalski, and T. Werner, Comput. Phys. Commun. **46**, 379 (1987).

[16] J. Hubbard, Phys. Rev. Lett. **3**, 77 (1959); R. L. Stratonovich, Dokl. Akad. Nauk SSSR **115**, 1097 (1957).

[17] A. Gilbert and A. G. W. Cameron, Can. J. Phys. **43**, 1446 (1965).

[18] T. von Egidy, H. H. Schmidt, and A. N. Behkami, Nucl. Phys. **A481**, 189 (1988); Till von Egidy and Dorel Bucurescu, Phys. Rev. C **72**, 044311 (2005); **73**, 049901(E) (2006).